Impact of Cloud Analysis on Numerical Weather Prediction in the Galician Region of Spain

M. J. SOUTO, C. F. BALSEIRO, AND V. PÉREZ-MUÑUZURI

Group of Nonlinear Physics, Faculty of Physics, University of Santiago de Compostela, Santiago de Compostela, Spain

M. XUE

School of Meteorology and Center for Analysis and Prediction of Storms, The University of Oklahoma, Norman, Oklahoma

K. BREWSTER

Center for Analysis and Prediction of Storms, The University of Oklahoma, Norman, Oklahoma

(Manuscript received 24 April 2001, in final form 10 June 2002)

ABSTRACT

The Advanced Regional Prediction System (ARPS) is applied to operational numerical weather prediction in Galicia, northwest Spain. The model is run daily for 72-h forecasts at a 10-km horizontal spacing. Located on the northwest coast of Spain and influenced by the Atlantic weather systems, Galicia has a high percentage (nearly 50%) of rainy days per year. For these reasons, the precipitation processes and the initialization of moisture and cloud fields are very important. Even though the ARPS model has a sophisticated data analysis system (''ADAS'') that includes a 3D cloud analysis package, because of operational constraints, the current forecast starts from the 12-h forecast of the National Centers for Environmental Prediction Aviation Model (AVN). Still, procedures from the ADAS cloud analysis are being used to construct the cloud fields based on AVN data and then are applied to initialize the microphysical variables in ARPS. Comparisons of the ARPS predictions with local observations show that ARPS can predict very well both the daily total precipitation and its spatial distribution. ARPS also shows skill in predicting heavy rains and high winds, as observed during November 2000, and especially in the prediction of the 5 November 2000 storm that caused widespread wind and rain damage in Galicia. It is demonstrated that the cloud analysis contributes to the success of the precipitation forecasts.

1. Introduction

Located in northwest Spain and influenced by Atlantic weather systems, Galicia has a high percentage (nearly 50%) of rainy days per year. The monthly mean number of days with precipitation of 1 mm or more, and the annual average (last column) measured at five different sites marked as A, B, C, D, E in Fig. 1c for the period 1961–90 are shown in Table 1. One can see that between October and May nearly all locations have rain on more than one-half of the days.

Galicia is located in a region of complex terrain and a wide variation in land use. Two typical synoptic situations exist in the region (Mounier 1964, 1979). In the summer, the region is primarily affected by the Azores high pressure center, with associated northwesterly winds and clear skies. In the winter, it is mainly affected by cold fronts associated with the low pressure center typically located over Great Britain. Ahead of the front, southwesterly winds are found. Convective precipitation is not common in the region, with heavy convective precipitation occurring on only a few days per year. In the winter season, the precipitation in this area is influenced largely by the passage of cold fronts from the Atlantic Ocean and the interaction of these systems with local topography. The fronts are usually associated with extratropical cyclones whose centers are generally located farther north. The topography of this region is shown in Fig. 1, where one can see the wide variation in terrain on small scales. For example, there is a mountain chain located in the southeast, only 200 km from the coast, with peaks of more than 1600 m. There are also elevations of about 500 m located in the northern part of the region just 20 km from the coast. The coastal bays, called rias, that characterize the southwest coastline have a strong influence on the local weather.

For these reasons, detailed forecasts of precipitation would be quite useful for this region, and we seek to investigate the forecasting of rainfall using a high-resolution nonhydrostatic numerical model and to study

Corresponding author address: Dr. M. J. Souto, Group of Nonlinear Physics, Faculty of Physics, University of Santiago de Compostela, E-15706 Santiago de Compostela, Spain.
E-mail: uscfamsa@cesga.es

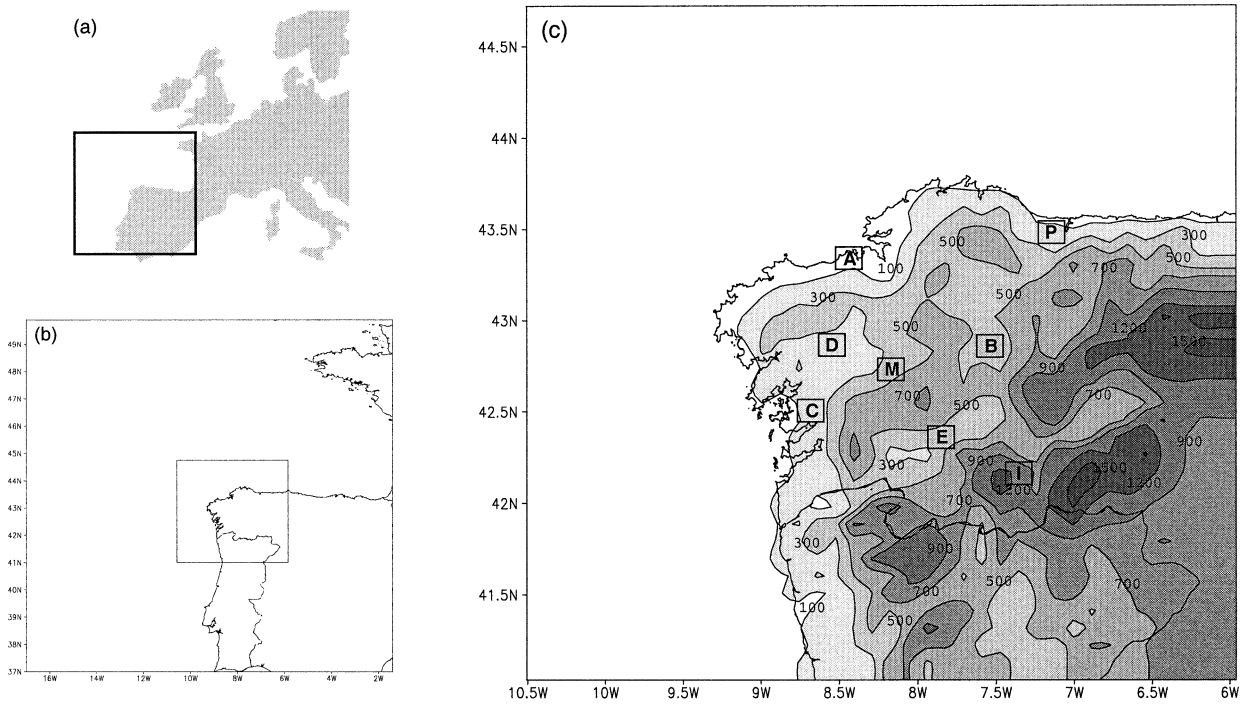

FIG. 1. (a) A 50-km coarse grid located on a Europe map, (b) 10-km ARPS grid located in coarse grid, and (c) ARPS topography on the 10-km grid. Contours and gray shading contrasts at 0, 100, 300, 500, 700, 900, 1200, and 1500 m. Monthly median precipitation is given in Table 1 for stations A–E and comparison of forecast and observed daily total precipitation is given in Fig. 12 for stations marked as M, I, and P.

the impact of the moisture and cloud initialization on model performance. Several studies have suggested that mesoscale models run at high resolutions can realistically predict precipitation over complex terrain (Bruintjes et al. 1994; Colle and Mass 1996; Gaudet and Cotton 1998; Colle et al. 1999; Buzzi et al. 1998; Sandvik 1998).

Initialization of cloud water content in a high-resolution numerical model is a significant issue and so far, most numerical weather prediction (NWP) models do not initialize it using observations. The simplest procedure for initializating cloud water is to start with zero values at all grid points and let the model gradually build up cloud mass. Thus, the model must ''spin up'' or create cloud water/ice during the first few hours. This creates a lag in the development of precipitation as the air must reach saturation, or nearly so when a cumulus parameterization scheme is employed, before precipitation can occur. Models that include cloud water as a prognostic variable may carry the field (from forecast background) in the data analysis process into the next prediction cycle. Without the use of additional information, such forecast fields may be in error, however. One previous study (Kristjánsson 1992) concluded that the initialization of the cloud water field by itself does not have a large effect on the spinup of precipitation and clouds, and a much larger effect is obtained when the humidity field is enhanced (described later in section 4). In Colle et al. (1999), when the fifth-generation Pennsylvania State University–National Center for Atmospheric Research Mesoscale Model (MM5) was initialized with a cold start (i.e., no hydrometeors and significant ageostrophic motions) it took 12–18 h on average for the model precipitation to spin up. To bypass the spinup issue, Colle and Mass (2000) only discussed results in the 8–44-h range when the model has been

TABLE 1. Monthly mean number of days with precipitation of 1 mm or more and the annual mean numbers (last column) measured at five different sites (A, B, C, D, E, as indicated in Fig. 1c).

	No. of precipitation days (1 mm+)												
Site	Jan	Feb	Mar	Apr	May	Jun	Jul	Aug	Sep	Oct	Nov	Dec	Annual
A	17.3	16.7	16.5	16.6	15.3	9.8	7.1	8.7	10.2	15.0	17.2	17.4	167.8
B	18.9	18.0	18.0	16.4	16.5	10.1	8.6	9.8	13.0	15.9	18.4	19.1	182.7
C	16.3	16.3	15.1	13.1	14.5	8.5	6.0	6.0	9.6	12.8	14.3	15.9	148.4
D	18.2	17.3	16.6	15.8	15.6	9.6	6.4	7.4	10.1	14.7	16.6	16.7	165.0
E	14.2	13.9	12.7	13.1	12.2	6.8	4.2	4.3	6.2	11.9	12.1	14.4	126.0

reasonably spun up. The effects of grid spacing, vertical resolution, and five different microphysical schemes on the precipitation forecasts were studied in their paper.

In recent years, most operational NWP centers have developed, or are developing, advanced data assimilation systems based on optimal interpolation, three-dimensional variational data assimilation (3DVAR) and four-dimensional variational data assimilation (4DVAR) techniques, with limited success in assimilating cloud and precipitation data. For example, only radiosonde humidity data are presently used operationally by the High-Resolution Limited-Area Model (HIRLAM), and are assimilated by optimal interpolation (OI; Amstrup and Huang 1999). At Météo-France, the operational embedded limited area model ALADIN and global NWP model ARPEGE (Action de Researche Petite Echelle Grande Echelle) currently use a 3DVAR system and use only radiosondes and the High Resolution Infrared Radiation Sounder (HIRS-11/12) humidity information in their upper-air assimilation (Courtier et al. 1991). Also, the 4DVAR has been operational at Météo-France for its global model since June 2000. Surface humidity data are used for the assimilation of surface prognostic quantities. The Eta Model of the National Centers for Environmental Prediction (NCEP) in the United States has used 3DVAR since February 1998. The model has prognostic cloud water and it is passed on from previous analysis times through the EDAS (Eta Data Assimilation System) cycle. It uses radiosonde data, surface reports, and satellite-based measurements of total column water vapor in the analysis. The system performs direct assimilation of Geostationary Operational Environmental Satellite (GOES) and polar satellite radiances in the 3DVAR and uses observed hourly precipitation and cloud-top pressure in its 3-hourly cycle. At the National Center for Atmospheric Research (NCAR), a recent investigation explores the impact of the assimilation of satellite-retrieved soundings on forecast error in the MM5: combinations of conventional surface and radiosonde observations and retrieved temperature and moisture soundings from polar-orbiting satellites are assimilated employing the four-dimensional data assimilation technique (Powers and Gao 2000). At NCEP, satellite-retrieved rainfall is assimilated into its Medium-Range Forecast (MRF) model (Falkovich et al. 2000) using the NCEP Global Data Assimilation System (GDAS; Zapotocny et al. 2000). Observations are inserted into the system every 6 h. At the European Centre for Medium-Range Weather Forecasts (ECMWF), 4DVAR was implemented in November 1997. Work has been done on the problem of cloud analysis in the context of advanced variational data assimilation. For example, in Janiskova (2001), one-dimensional variational data assimilation (1DVAR) experiments using simulated observations were performed to investigate the potential of radiation and cloud schemes to modify model temperature, humidity, and cloud profiles to produce a better match to the observations of radiation fluxes. Feasibility studies in a 1DVAR framework using data from field experiments that measure both cloud properties and radiative fluxes have also been carried out.

At the Center for Analysis and Prediction of Storms (CAPS) at The University of Oklahoma, in order to provide detailed initial conditions for moisture variables in the Advanced Regional Prediction System (ARPS; Xue et al. 1995, 2000, 2001), and to serve as the basis for moisture data assimilation, a cloud analysis procedure has been developed within the ARPS Data Analysis System (ADAS; Brewster 1996). The cloud initialization procedure is a customization of the algorithms used by the National Oceanic and Atmospheric Administration (NOAA) Forecast Systems Laboratory in the Local Analysis and Prediction System (LAPS; Albers et al. 1996) with certain enhancements and refinements (Zhang et al. 1998; Zhang 1999). It incorporates cloud reports from surface stations reporting World Meteorological Organization (WMO) standard aviation routine weather reports (METARs), satellite infrared and visible imagery data, and radar reflectivity to construct three-dimensional cloud and precipitation fields. The products of the analysis package include three-dimensional cloud cover, cloud liquid and ice water mixing ratios, cloud and precipitation types, in-cloud vertical velocity, icing severity index, and rain/snow/hail mixing ratios. Cloud base, cloud top, and cloud ceiling are also derived.

In this work, ARPS application to an operational numerical weather forecast for Galicia, Spain, is described. Even though the ARPS model has ADAS, a sophisticated data analysis system that includes a three-dimensional cloud analysis package, because of operational constraints, our current forecast starts from the 12-h forecast from the NCEP Aviation Model (AVN). Still, procedures from the ADAS cloud analysis are being used to construct the cloud fields based on AVN forecast data, and a three-category ice microphysics scheme is used in the ARPS operational runs. The next section describes the operational implementation, and the governing equations are presented in section 3. The cloud analysis procedure is explained in section 4; sections 5 and 6 present and summarize the results.

2. Operational implementation

The ARPS is applied to an operational numerical weather forecast for Galicia, Spain. The ARPS model was chosen because its nonhydrostatic dynamics, generalized terrain-following coordinate, and nesting capabilities are well suited for the complexities of the Galician region. ARPS had also been tested quasi-operationally for several years, especially for convective seasons, at CAPS (Droegemeier et al. 1996; Xue et al. 1996; Carpenter et al. 1999). For this application, the nesting was set up to permit the resolution of flows at two scales: the influence of local terrain features in the 10-km fine grid, and the mesoscale circulations (particularly those concerning the passage of cold fronts from

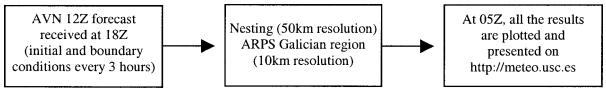

FIG. 2. Scheme of the daily operational forecast for the Galician region.

the Atlantic Ocean) by the 50-km coarse grid. The principal steps in the production of the daily 72-h forecast are depicted schematically in Fig. 2. The ARPS model starts from an enhanced 12-h forecast of the NCEP AVN model and uses the boundary conditions also obtained from the NCEP AVN model at a 3-h interval on a coarse grid covering a 1500 km × 1500 km area (Fig. 1b). A fine grid covering a 400 km × 400 km area (Fig. 1c) is nested within the coarse domain. There are 43 sigma-z levels in the vertical extending to 21 km. The fine grid uses its own higher-resolution terrain with a gradual transition to the coarse-grid terrain in a boundary zone to improve the match between solutions. The initial condition of the coarse grid is interpolated to fine-grid grid points using linear and quadratic interpolation in the vertical and horizontal, respectively. The 12-h AVN forecast is used because of operational time constraints. We do not receive the AVN dataset until 7 h after analysis time. It is not possible for us to use the AVN analysis and observations and still be able to run the nested models and produce forecasts for the same day. The forecast had to be available at the first hour in the morning (0600 local standard time). In the future we plan to run the model twice daily, using the 0-h and 12-h AVN output. Forecasts on the two grids take approximately 8 h of CPU time on a Fujitsu VPP300E computer using the sole processor available to the project. Adding the time needed for plotting and Web posting, the process takes a total of 10 h. The forecasts for the present day, the next day, and the subsequent day are ready for the weather forecasters and general public on the Galician regional forecast Web site (http://meteo.usc.es) at about 0500 UTC daily (i.e., 0600 local standard time).

3. The governing equations

The governing equations of the ARPS include conservation equations for momentum, heat, mass, water substance (water vapor, liquid, and ice), subgrid-scale (SGS) turbulent kinetic energy (TKE), and the equation of state of moist air. The modified three-category ice scheme of Lin et al. (1983) is used for microphysics parameterization. It includes two liquid phases (cloud and rain) and three ice categories (ice cloud, snow, and hail or graupel). The implementation of the Lin scheme follows that of Tao and Simpson (1993) and includes the ice-water saturation adjustment procedure of Tao et al. (1989). The source terms corresponding to the conservation equation of water subtances q_c (cloud water), q_r (rain), q_i (cloud ice), q_s (snow), and q_h (hail/graupel) include the following conversion terms based on

$$S_{q_c} = \rho(c - e_c) - T_{q_c}, \tag{1}$$

$$S_{q_r} = \rho(-e_r + m_s + m_h - f_s - f_h) - T_{q_r}, \tag{2}$$

$$S_{q_i} = \rho(d_i - s_i) - T_{q_i}, \tag{3}$$

$$S_{q_s} = \rho(d_s - s_s - m_s + f_s) - T_{q_s}, \text{ and} \tag{4}$$

$$S_{q_h} = \rho(d_h - s_h - m_h + f_h) - T_{q_h}. \tag{5}$$

The symbols c, e, f, m, d, and s denote the rates of condensation, evaporation of droplets, freezing of raindrops, melting of snow and graupel, deposition of ice particles, and sublimation of ice particles, respectively. Specific species are identified by the subscripts, with c, r, i, s, and h representing cloud, rain, ice, snow, and hail, respectively. The terms T_{q_c}, T_{q_r}, T_{q_i}, T_{q_s}, and T_{q_h} are microphysical transfer rates between the hydrometeor species, and their sum is zero. The complicated transfers encompass nearly 30 processes. They include autoconversion, which parameterizes the collision–coalescence and collision–aggregation, and accretion among the various forms of liquid and solid hydrometeors. The transformation of cloud ice to snow through autoconversion (aggregation), the Bergeron processes (Bergeron 1935), and subsequent accretional growth or aggregation to form hail are simulated. Hail is also produced by various contact mechanisms and via probabilistic freezing of raindrops. Evaporation (sublimation) is considered for all precipitation particles outside the cloud. The melting of hail and snow, wet and dry growth of hail, and shedding of rain from hail are included. The complete formulation of each of the transfers can be found in Lin et al. (1983). More details on the model formulation can be found in Xue et al. (1995, 2000).

4. Cloud analysis procedure

For our purposes, a three-dimensional background cloud cover field on the 50-km coarse grid is derived from the relative humidity values in the initial and boundary condition fields using an empirical power relationship similar to one used in Koch et al. (1997):

$$\mathrm{CF} = \left(\frac{\mathrm{RH} - \mathrm{RH0}}{1.0 - \mathrm{RH0}}\right)^b. \tag{6}$$

Here, CF is the cloud fractional cover that ranges from 0.0 to 1.0, RH is the relative humidity, RH0 is a relative humidity threshold whose value is dependent on the height, and b is an empirical constant. In this case, b is set to 2. The relationships between cloud cover and RH as a function of height z used in this work are depicted in Fig. 3.

After the three-dimensional cloud-cover distribution is obtained, values for the various cloud species are calculated using the same procedures employed in the ADAS cloud scheme for regions where directly observed cloud information is lacking. The procedure follows modified LAPS cloud scheme (Albers et al. 1996)

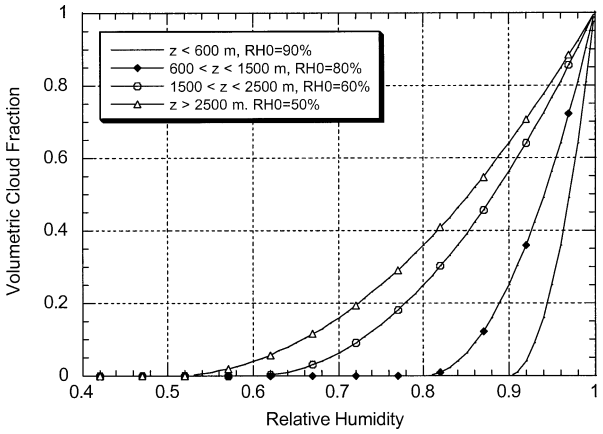

FIG. 3. Relationship between cloud cover and relative humidity at different height levels. (Reproduced from Zhang 1999.)

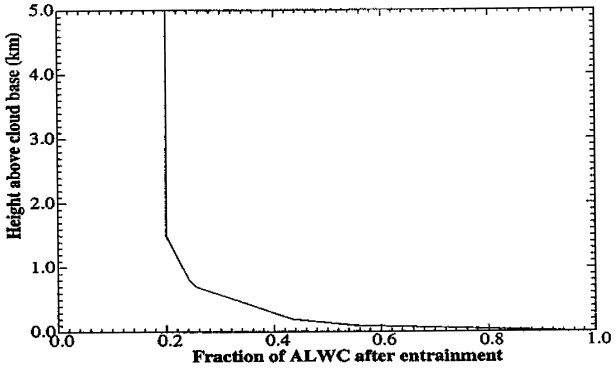

FIG. 4. Entrainment reduction curve. (Reproduced from Zhang 1999.)

as is given in Zhang et al. (1998) and Zhang (1999). For each grid column, cloud tops and bases are determined for layers having a cloud coverage that exceeds a threshold value (0.5 in this case). The adiabatic liquid water content (ALWC) is the maximum value of liquid water content in the cloud based solely on thermodynamic processes, taking into account the change in liquid water due to the change in the saturation mixing ratio. ALWC is estimated by assuming moist adiabatic conditions throughout the cloud and is calculated for each grid point (and accumulated) from cloud base upward. This adiabatic computation of LWC consists of several steps. From cloud base, the moist adiabatic lapse rate is used to calculate the temperature in 50-m increments above cloud base. These temperatures define the saturation vapor pressures at 50-m increments throughout the cloud. The difference in saturation vapor pressure over a 50-m interval defines the additional condensed moisture that is accumulated beginning at cloud base and continuing to the cloud top. Then an entrainment reduction curve (Fig. 4) is applied, which reduces the ALWC by 40% near the cloud base and by 75% at about 500 m above the cloud base. Constant 80% reduction is applied for levels 1.5 km or more above the cloud base. The reduced ALWC is defined as cloud liquid water when temperature is warmer than $-10°C$, and as cloud ice when temperature is colder than $-30°C$. A linear ramp is applied for the temperature in between. The specific humidity at those grid points that contain cloud water is saturated, so that the conditions for cloud formation in the condensation scheme of the model are satisfied.

Last, a latent heat adjustment to temperature based on added ALWC (ΔT) is applied, according to the formula

$$\left.\begin{aligned} \Delta T_{q_c} &= a\Delta q_c, \qquad a = f_{q_c}L_v/C_p \\ \Delta T_{q_i} &= b\Delta q_i, \qquad b = f_{q_i}(L_v + L_f)/C_p \end{aligned}\right\} \qquad \Delta T = \Delta T_{q_c} + \Delta T_{q_i}, \tag{7}$$

where f_{q_c} and f_{q_i} are constants for adjusting the fraction of latent heat added from q_c and q_i, respectively (in this case, 0.8), L_v and L_f are the latent heat of vaporization and fusion at 0°C, respectively, and C_p is the specific heat of dry air at constant pressure.

5. A representative case

The period from November 2000 to mid-February 2001 was characterized by very inclement weather over Galicia. Active cold fronts coming from the Atlantic Ocean caused very strong southwesterly winds with heavy rains over the entire region, especially in the southwest because of orography. During this period, Galicia experienced 20 days of severe weather, including warnings for severe rain and wind. A wind warning is issued when the mean wind velocity in the coastal areas is higher than 80 km h^{-1} (22 m s^{-1}), and a rain warning is issued when precipitation greater than 30 mm is accumulated in 1 h or 60 mm in 12 h. Galicia is not a very large region, but it has a very complex topography that influences the spatial distribution of precipitation. This fact complicates the precipitation forecast. In Fig. 5, one can see large differences among total accumulated precipitation measurements (numbers in the boxes) for November 2000 depending on the location. High values of precipitation exceeding 900 mm accumulated in the southwest where moist air from the sea flows over the mountains. By contrast, just over 100 mm accumulated in the northeast part of Galicia in a region of rain shadowing due to terrain. The ability of the forecast model to replicate the dis-

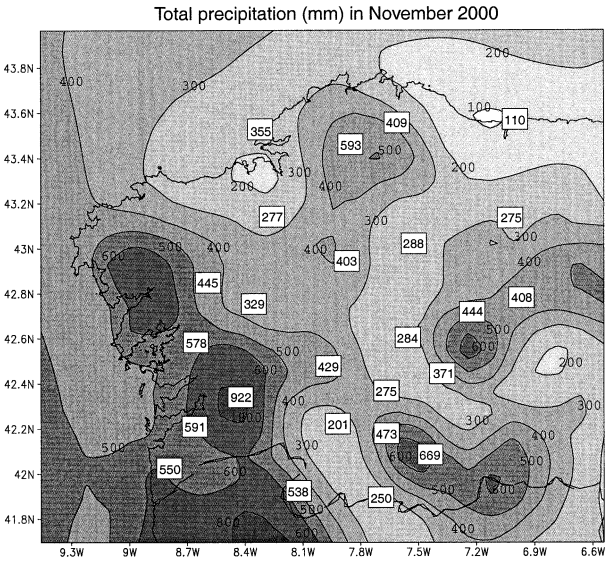

FIG. 5. Comparison of total precipitation over Galicia during Nov 2000 as measured (numbers in boxes) and that predicted by ARPS using cloud water analysis (contours and gray shading contrasts at 100, 200, 300, 400, 500, 600, and 800 mm).

parate precipitation regimes in this figure will be addressed in later sections.

In this work, we present the results obtained with the ARPS model and demonstrate the importance of the cloud initialization for the Galician operational forecast in a period of severe weather—not only in the daily total precipitation but also in its spatial distribution. For brevity, we present here the results for November 2000, and particularly, the storm that occurred on 5 November 2000. The synoptic situation for that day is shown in Fig. 6, which is taken from the National Weather Service of Spain (INM) bulletins. A cold front associated with a deep low centered on the southwest of the British Isles passed through Galicia, causing strong southwesterly winds and heavy rains over the entire region. This situation can be considered as representative of the general synoptic pattern during the entire month of November 2000. This synoptic pattern was well described by ARPS, as shown in Fig. 7, where sea level pressure (contours) and 850-hPa temperature (shaded field) predicted by ARPS (0–24-h forecast) on the 50-km coarse grid for 5 November 2000 at 0600, 1200, and 1800 UTC are shown: the ARPS model predicted quite well the location of both cold and warm fronts as compared with the analysis in Fig. 6.

As shown in Fig. 6, at 1200 UTC 5 November 2000 the cold front is just arriving in northwest Galicia, a cold front with a band of cumulonimbus convection along it. This situation was well predicted by ARPS. As is shown in Fig. 8a, ARPS predicted a band of high vertically integrated rainwater mixing ratio (q_r) at the observed frontal location, in the run where the cloud generation at the initial and boundary conditions is included. Without the cloud analysis, the model was not able to predict the frontal precipitation, so the q_r values obtained at the same time are smaller throughout the domain, especially in the northwest corner near the front. (Fig. 8b).

In Fig. 9 the surface wind field forecast by the ARPS model for 1500 UTC 5 November 2000 is shown. The model produced strong southwesterly winds, with values around 20 m s^{-1} in the northern coastal areas (wind gusts higher than 30 m s^{-1} were measured in coastal towns). A comparison between observed and forecast wind velocity and direction for 5 November 2000 is shown in Fig. 10 for two locations marked in Fig. 1 as A (on the west coast, 5-m elevation) and B (in the southeast mountains, 970-m elevation). The ARPS model predicted the observed increase in wind velocity in the afternoon and maintained the southwesterly winds all day at both locations.

6. Verification

The Galician meteorological network, consisting of 43 climatological stations and 22 meteorological surface

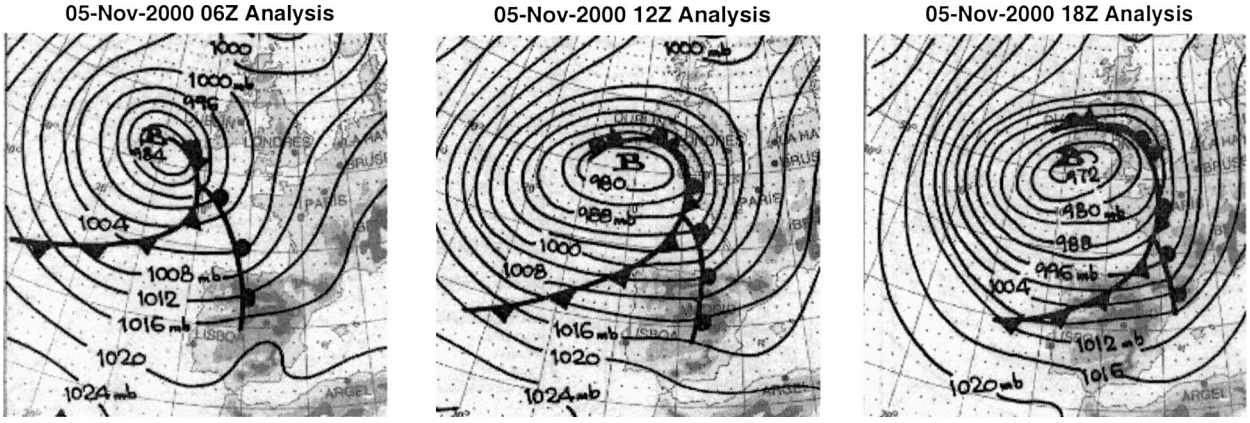

FIG. 6. Synoptic analysis for 5 Nov 2000 at 0600, 1200, and 1800 UTC. Sea level pressure is shown in hectopascals (4-hPa interval). The maps are adopted from National Weather Service of Spain (INM) bulletins. Here, the B symbol indicates the low pressure center, derived from the Spanish word baja.

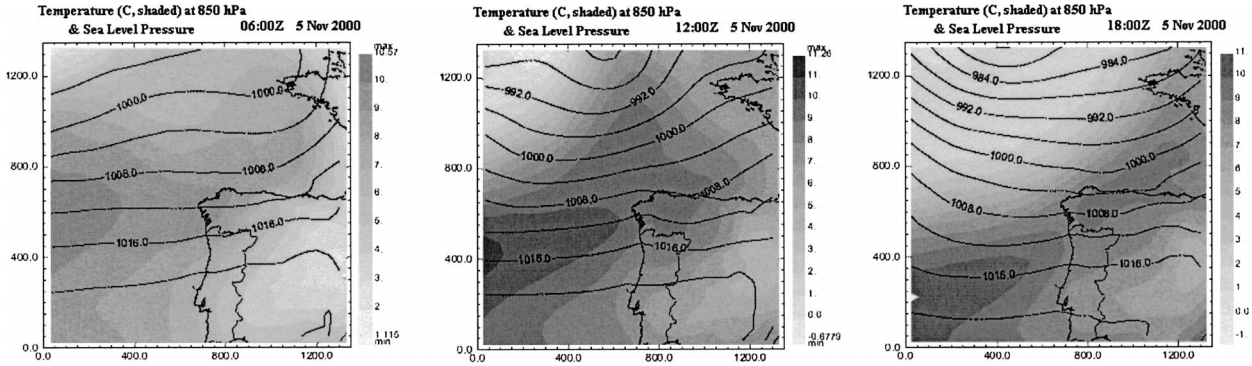

FIG. 7. Sea level pressure (4-hPa contours) and 850-hPa temperature (shaded field) predicted by ARPS on 50-km coarse grid for 5 Nov 2000 at 0600, 1200, and 1800 UTC.

stations covering the entire region, was used to verify the model forecasts. In Fig. 5 (shown earlier), the total rainfall predicted with the ARPS model for the month of November is contoured and compared with observations (numbers in boxes). ARPS forecasts using cloud analysis agree quite well with the observations not only in quantitative amount but also in the geographical distribution. ARPS predicted very high values of precipitation in the southwest area of the region, where moist air from the sea is brought in by the southwest winds (see Fig. 9) to be lifted over the topography. These values of precipitation are greater than 800 mm, very close to the measurement maximum of 922 mm. In the mountainous areas of the southeast, the model also predicted the high values of precipitation measured, around 600 mm, and correctly distinguished the valley zones with values of only 200 mm. In the north part of the region, the model also produced a good forecast and reproduced the significant precipitation (593 mm) that occurred in the mountainous area located in the center, and the drier zones on each side of this mountain. The forecast of 100 mm from ARPS in the northeast compares quite well to the measured minimum value of 110 mm there. On the other side, in the northwest, the ARPS-predicted precipitation of around 250 mm there also agrees quite well to the measured values.

Focusing on a particular day, we can see more clearly the importance of the cloud analysis in the precipitation forecast. In Figs. 11a and 11b the total rainfall predicted with and without cloud analysis, respectively, is compared with measurements (numbers in boxes) for 5 November 2000. At first glance, there is an important difference in the values obtained over the sea: with the cloud analysis (Fig. 11a) a more realistic distribution is

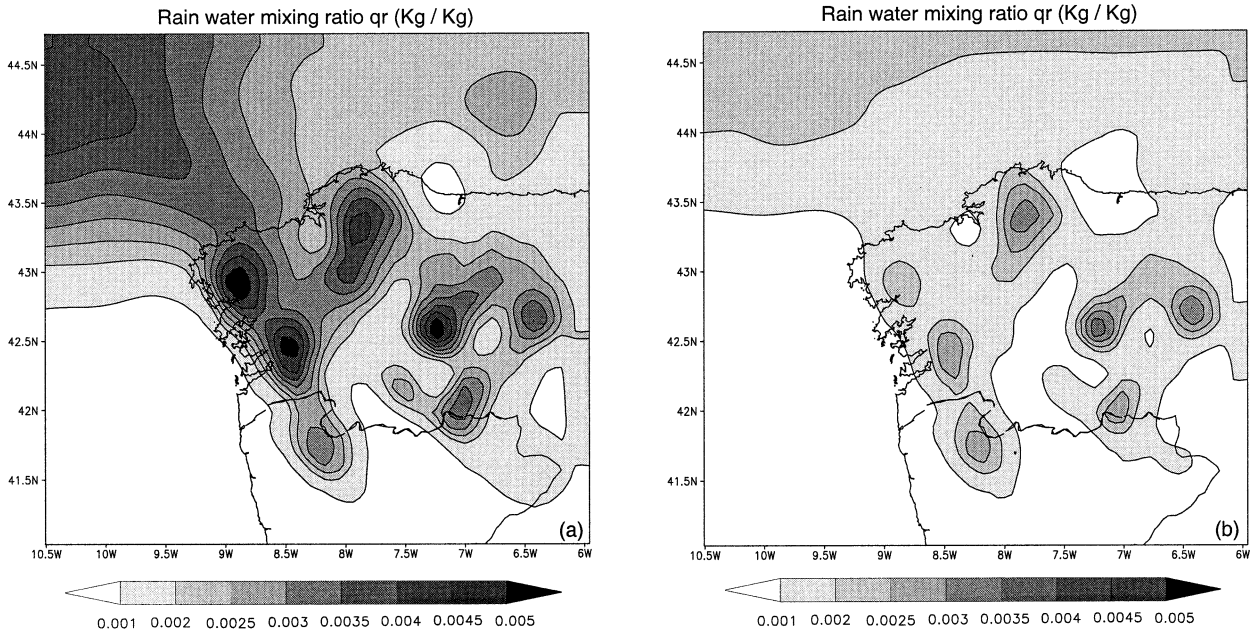

FIG. 8. Vertical integrated rainwater mixing ratio (q_r) predicted with ARPS on the fine grid at 1200 UTC 5 Nov 2000 (a) with and (b) without cloud analysis. The model started from 0000 UTC 5 Nov initial condition based on the 12-h AVN forecast background.

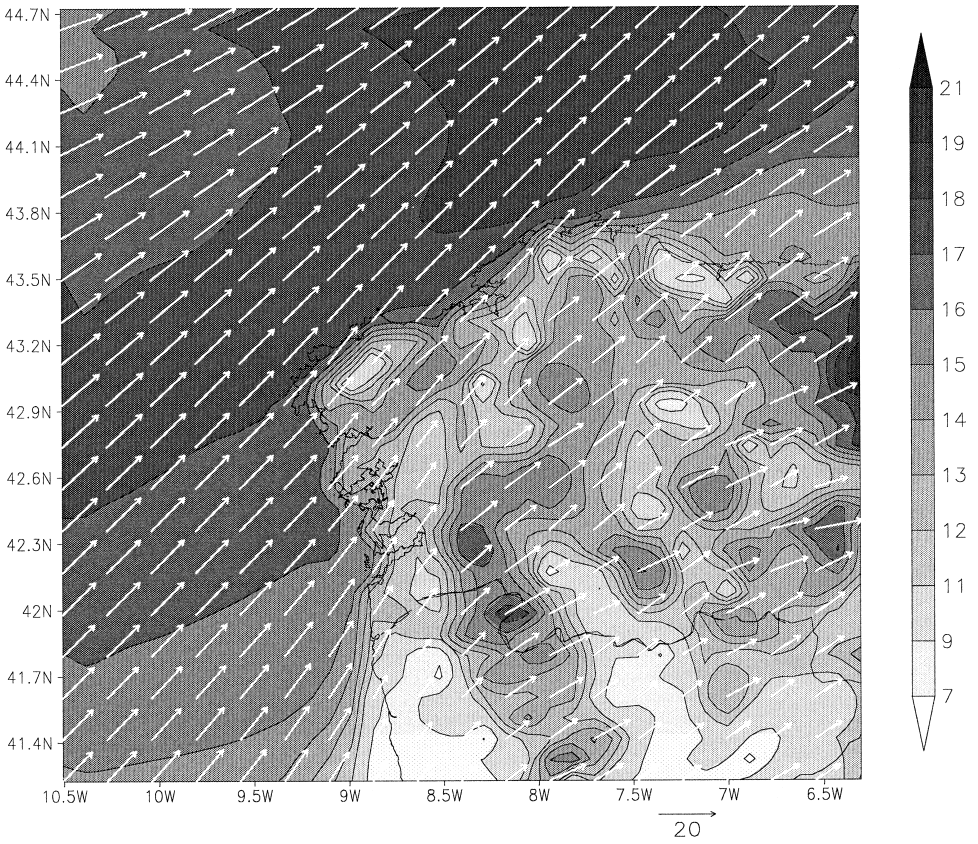

FIG. 9. Surface wind velocity (shaded) and wind direction (vectors) predicted by ARPS on 10-km fine grid at 1500 UTC 5 Nov 2000.

obtained, because it shows significant rainfall values in the west, where the cold front was; however, without it (Fig. 11b) the model does not represent correctly the frontal clouds, and it generates less rainfall. Although the rainfall spatial distribution over the terrain is similar in both cases, the quantitative forecast is better in Fig. 11a, as we can see, for example, in the mountainous area of the north, where 118 mm was measured and the predicted value was near 110 mm, while in Fig. 11b the predicted value was about 80 mm. Also, in the mountainous area of the southeast, 116 and 78 mm were measured at neighboring points and ARPS predicted values in Fig. 11a of 119 and 89 mm, respectively; in Fig. 11b the model-predicted precipitation was less than 80 mm. An accurate forecast of the rainfall maxima is very important for alerting the public about the threat of heavy rainfall.

The daily total precipitation predicted by ARPS with and without cloud analysis for November 2000 is compared with measurements at three representative surface stations in Fig. 12. We consider them to be representative because they are located at very different locations in the region and at different elevations: MOUR (Mouriscade, Pontevedra, 490 m), INVE (Invernadeiro, Ourense, 1020 m), and PMUR (Pedro Murias, Lugo, 43 m) (M, I, P in Fig. 1, respectively). With cloud analysis, the model was able to follow the daily evolution of the precipitation remarkably well and to distinguish with accuracy the heavy and light rain days. When the cloud analysis is not applied, the rain forecast obtained for heavy rain days is typically lower than measurements. It is interesting to note the important differences between station INVE, located in the southeast mountainous area of Galicia and having only 1 day of no precipitation and a daily mean value of about 25 mm, and station PMUR, located on the coast, in the northeast portion of the region and having 8 days of no precipitation and a daily mean value of only 4 mm. The model appears to have good skills in reproducing these differences. It is also shown in Fig. 13 that in the precipitation time series (predicted and measured) at the MOUR location for 5 November 2000, with the cloud analysis applied at the initial conditions and cloud water enhancement in the (AVN forecast) boundary conditions, the predicted values agree quite well with measurements during the entire 24-h time period.

In Fig. 14, the scattergram plots of observed precipitation (mm) and forecasts for 5 November 2000 with and without cloud analysis summarize the model precipitation performance: light precipitation is well predicted in both cases but the cloud analysis improved the heavy precipitation forecast significantly. For values ex-

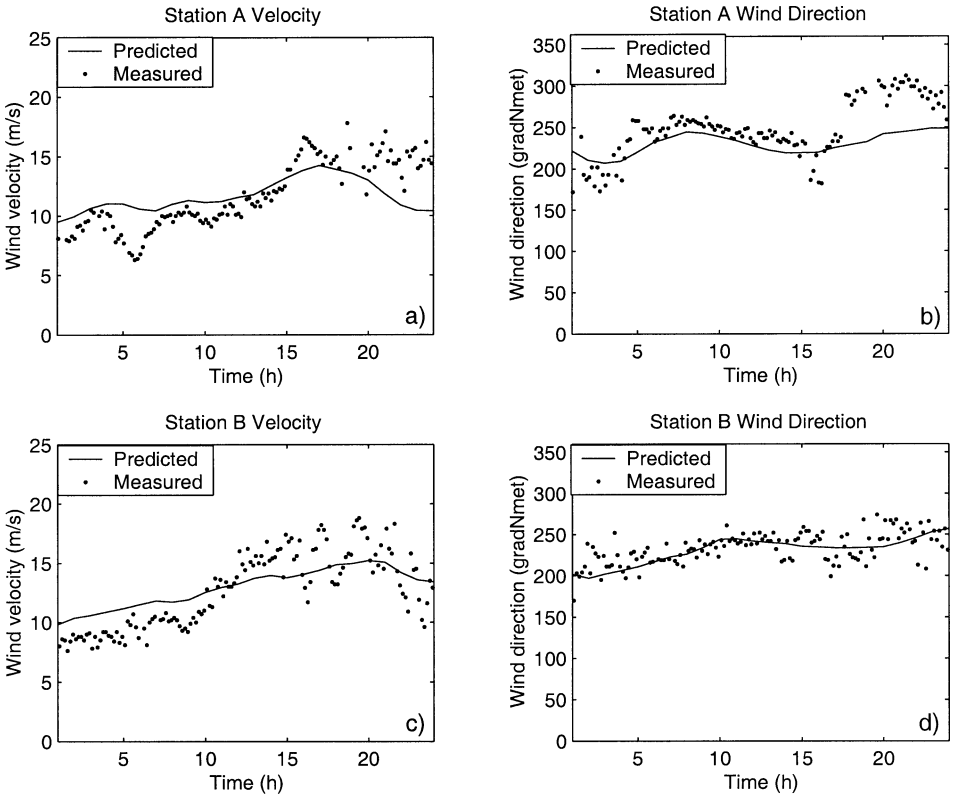

FIG. 10. Surface wind speed and direction comparison between measurements at (a), (b) A (on the west coast, 5 m) and (c), (d) B (in the southeast mountains, 970 m) stations, and model results for 5 Nov 2000.

ceeding 60 mm, the precipitation without cloud analysis is significantly underpredicted while the case with cloud analysis produced a better fit between the forecast and observation. In general, the case without cloud analysis has a significant negative bias in precipitation amount, while the case with cloud analysis tends to slightly overpredict the precipitation although the absolute bias is smaller. The rmse values obtained are quite good and are slightly lower with cloud analysis than without it.

We further formally verify the precipitation forecasts using bias and equitable threat scores. The bias score $B = F/O$ is the ratio of the number of stations forecast to reach or exceed a certain precipitation threshold (F) to the number of stations that actually exceed the threshold (O); a perfect forecast would have $B = 1$, while values of B less than and greater than 1 represent underforecasting and overforecasting, respectively, of the precipitation areal coverage. A limitation of the bias score is

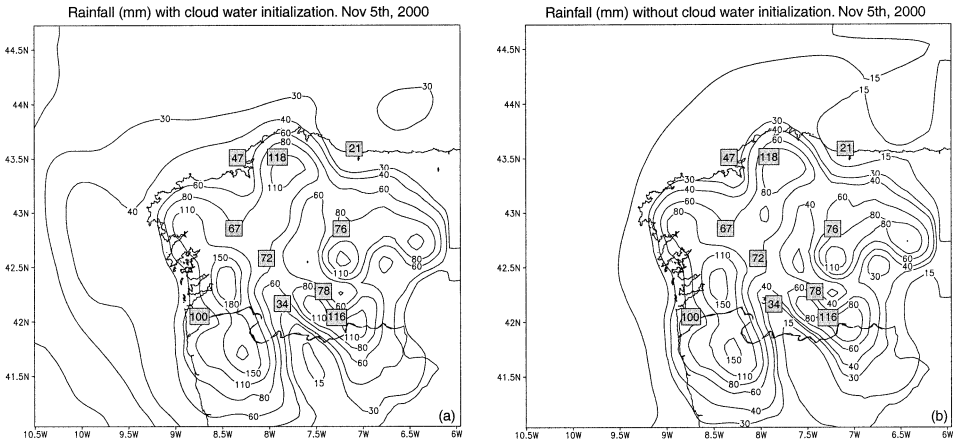

FIG. 11. Comparison between total rainfall over Galicia for 5 Nov 2000 predicted by ARPS (a) with and (b) without cloud analysis and observations (numbers in boxes).

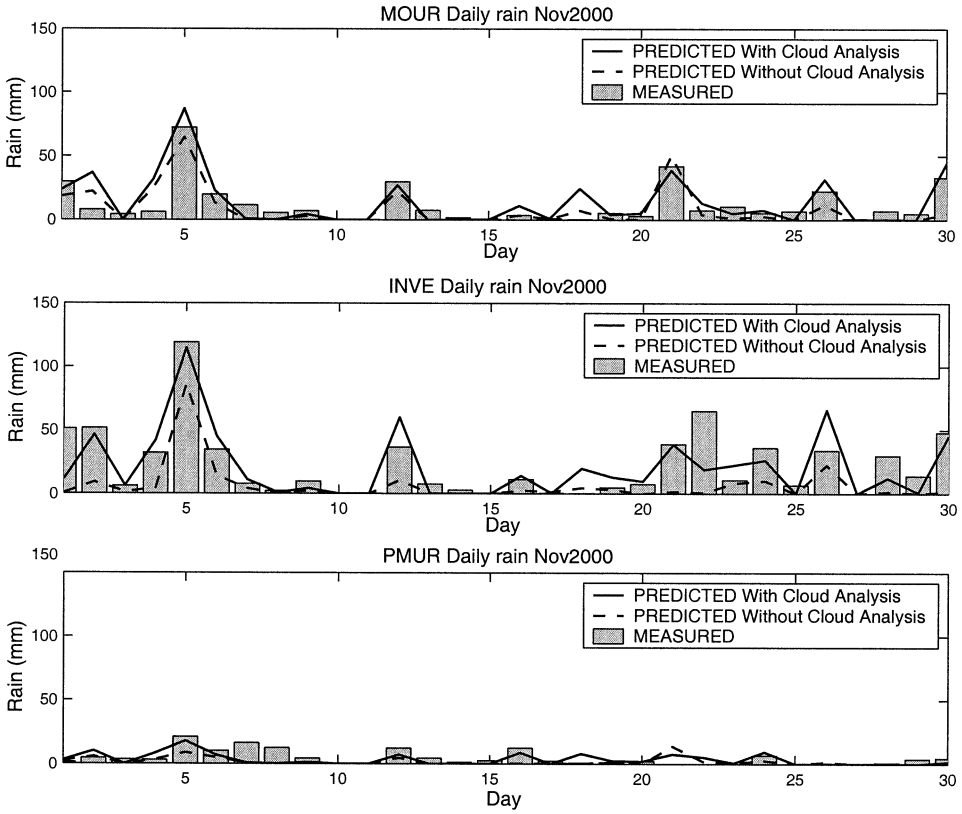

FIG. 12. Comparison of daily total precipitation measured (bars) and predicted by ARPS with (solid line) and without (dashed line) cloud analysis at stations (top) MOUR (42.61°N, 8.14°W), (middle) INVE (42.12°N, 7.34°W), and (bottom) PMUR (43.54°N, 7.08°W). These stations are marked M, I, and P in Fig. 1c.

that it does not provide a measure of the coincidence of stations for which precipitation was forecast with those at which it is observed; this can be measured through an equitable threat score T defined as

$$T = \frac{\mathrm{CF} - \mathrm{CH}}{F + O - \mathrm{CF} - \mathrm{CH}}, \quad \text{with CH} = \frac{FO}{N}, \quad (8)$$

where CF is the number of correctly forecast stations (both model and observations produce precipitation at or above a given threshold), CH is the number of correct forecasts that could be obtained at random, N is the number of points within the verification area, and F and O are as defined above (Schaefer 1990; Rogers et al. 1996). Table 2 contains these skill scores for November 2000. At low-precipitation thresholds (0.2 and 10 mm), both B and T values are close to 1, and they are exactly 1 for 5 November, when a significant storm occurred (precipitation values bigger than 100 mm were measured at different locations). For this day, the model slighty overestimated the areal coverage of heavy rain (e. g., $B = 1.4$ for 40-mm threshold) and predicted quite well the geographical location ($T = 0.56$ for 50-mm threshold). Note that for all thresholds, the same 10 stations are being considered.

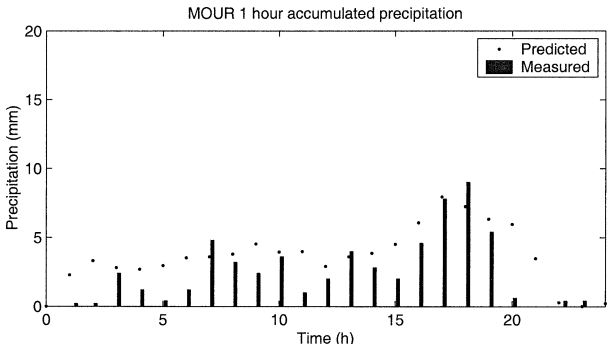

FIG. 13. The 1-h accumulated precipitation measured (black bars) and predicted (dots) at MOUR for 5 Nov 2000.

The comparison of monthly mean value of bias and equitable threat score with and without cloud analysis for various daily precipitation thresholds (mm) for November 2000 is shown in Fig. 15. For low thresholds, the results imply good skill for the rain/no-rain forecast and its location; for larger thresholds, the model loses some precision in the geographical location of the precipitation but maintains good bias scores. When the cloud analysis is applied, the B and T scores are improved for all thresholds, with the lone exception being 40 mm, at which the T score is about even with the forecast without cloud analysis.

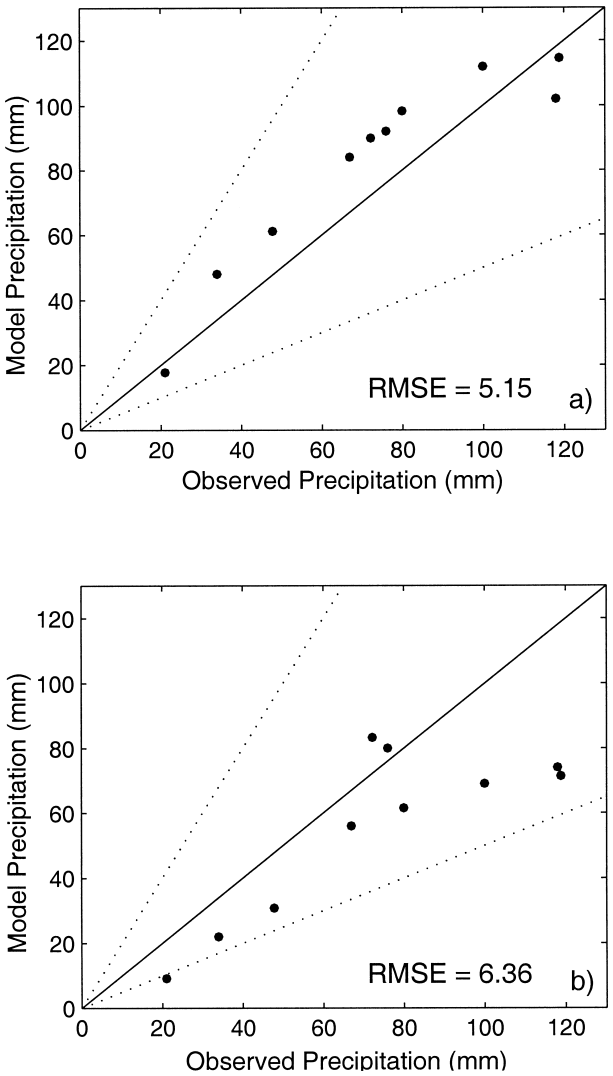

FIG. 14. Scatter diagrams of observed precipitation (mm) and model forecasts (a) with and (b) without cloud analysis for 5 Nov 2000. For reference, the 1-to-1 and 2-to-1 lines are shown as solid and dotted, respectively.

7. Summary and conclusions

The Advanced Regional Prediction System has been applied to operational numerical weather forecasts for Galicia, in northwestern Spain, since January 2000. Because of the high percentage of rainy days per year in this region, the precipitation processes and the initialization of clouds and moisture in the model are very important. Portions of the cloud analysis procedure within the ARPS Data Analysis System was used to construct the cloud fields based on forecast relative humidity from the global AVN model of NCEP. The cloud fields were used to initialize the microphysical variables in the ARPS. A three-category ice scheme that includes two liquid phases (cloud and rain) and three ice categories (ice cloud, snow, and hail or graupel) is used for microphysics parameterization in ARPS.

TABLE 2. Skill scores for ARPS model with cloud analysis at the meteorological stations. Labels on heading denote thresholds used to evaluate each score, in millimeters of precipitation. Only days with observed precipitation are shown.

	Bias				Equitable threat score			
Date	0.2	10.0	20.0	40.0	0.2	10.0	20.0	40.0
1 Nov	1.0	1.17	1.00	0.0	1.0	0.4	0.03	0.0
2 Nov	1.0	2.25	3.5	0.5	1.0	0.22	0.17	0.46
3 Nov	0.33	0.0	—	—	0.09	0.0	—	—
4 Nov	1.0	1.6	3.0	—	1.0	0.42	0.1	—
5 Nov	1.0	1.0	0.88	1.4	1.0	1.0	0.75	0.56
6 Nov	1.0	1.0	1.33	—	1.0	0.53	0.28	—
7 Nov	0.78	0.14	—	—	0.42	−0.07	—	—
8 Nov	0.63	0.0	0.0	—	0.42	0.0	0.0	—
9 Nov	1.0	0.0	—	—	1.0	0.0	—	—
10 Nov	0.0	—	—	—	0.0	—	—	—
12 Nov	1.0	0.89	0.88	—	1.0	0.74	0.75	—
13 Nov	0.0	0.0	—	—	0.0	0.0	—	—
14 Nov	0.75	—	—	—	0.19	—	—	—
15 Nov	2.0	—	—	—	0.19	—	—	—
16 Nov	1.0	3.5	—	—	1.0	0.0	—	—
17 Nov	1.6	—	—	—	0.27	—	—	—
18 Nov	1.6	0.0	—	—	0.42	0.06	—	—
19 Nov	1.0	0.25	—	—	1.0	−0.06	—	—
20 Nov	1.0	0.5	—	—	1.0	−0.05	—	—
21 Nov	1.0	1.0	1.17	4.0	1.0	1.0	0.75	0.19
22 Nov	1.0	2.0	0.0	0.0	1.0	0.12	0.0	0.0
23 Nov	1.0	2.0	—	—	1.0	0.46	—	—
24 Nov	1.0	1.25	0.0	—	1.0	0.72	0.0	—
25 Nov	0.6	0.0	—	—	0.49	0.0	—	—
26 Nov	1.0	1.0	1.5	—	1.0	1.0	0.61	—
28 Nov	0.67	0.0	0.0	—	0.53	0.0	0.0	—
29 Nov	0.29	0.0	—	—	0.17	0.0	—	—
30 Nov	1.0	0.83	0.5	0.0	1.0	0.74	0.36	0.0

Comparisons of the ARPS predictions with local observations show that both the daily total precipitation and its spatial distribution were predicted reasonably well. The latter is very challenging in this region, as is shown by the large spatial variations in the observed

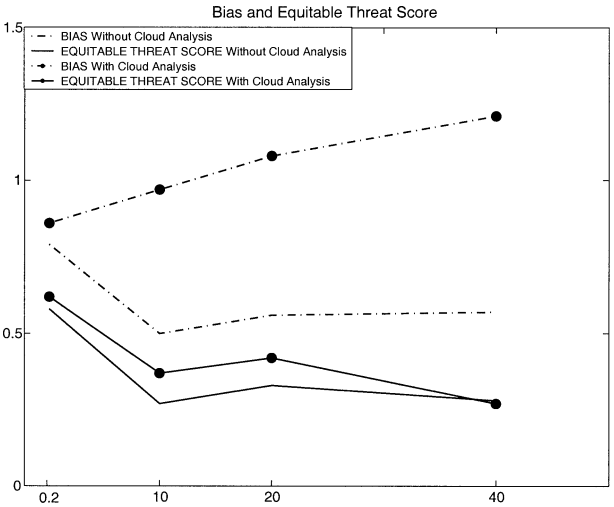

FIG. 15. Comparison of monthly mean bias and threat score for various precipitation thresholds (mm day^{-1}) for Nov 2000 with and without cloud analysis.

precipitation rates. ARPS also shows skill in predicting heavy rains and high winds, as were observed during most of November 2000 and exemplified by the prediction of the 5 November 2000 storm in Galicia. The model successfully reproduced the influence of the complex local terrain features and the mesoscale circulations that combine to produce the complex spatial distribution of rain in Galicia for this specific case as well as in the monthly values. It was also shown through individual cases, as well as month-long statistics, that both the precipitation pattern and amount were improved when the cloud analysis procedure is employed.

Acknowledgments. This work is supported by the Department of Environment of the Galician Government (Xunta de Galicia) as part of its Observational and Meteorological Forecasting Unit. Partial support by the Research Grant PGIDT01MAM20802PR (Xunta de Galicia) is also acknowledged.

REFERENCES

Albers, S. C., J. A. McGinley, D. A. Birkenheuer, and J. R. Smart, 1996: The Local Analysis and Prediction System (LAPS): Analysis of clouds, precipitation, and temperature. *Wea. Forecasting,* **11,** 273–287.

Amstrup, B., and X.-Y. Huang, 1999: Impact of the additional FASTEX radiosonde observations on the High-Resolution Limited-Area Model (HIRLAM) data-assimilation and forecasting system. *Quart. J. Roy. Meteor. Soc.,* **125,** 3359–3374.

Bergeron, T., 1935: On the physics of cloud and precipitation. *Proc. Fifth Assembly of IUGG,* Vol. 2, Lisbon, Portugal, Int. Union Geod. Geophys., 156–178.

Brewster, K., 1996: Implementation of a Bratseth analysis scheme including Doppler radar. Preprints, *15th Conf. on Weather Analysis and Forecasting,* Norfolk, VA, Amer. Meteor. Soc., 92–95.

Bruintjes, R. T., T. L. Clark, and W. D. May, 1994: Interactions between topographic airflow and cloud/precipitation development during the passage of a winter storm in Arizona. *J. Atmos. Sci.,* **51,** 48–67.

Buzzi, A., N. Tartagliones, and P. Malguzzi, 1998: Numerical simulations of the 1994 Piedmont flood: Role of orography and moist processes. *Mon. Wea. Rev.,* **126,** 2369–2383.

Carpenter, R. L. J., K. K. Droegemeier, G. M. Basset, S. S. Weygandt, D. E. Jahn, S. Stevenson, W. Qualley, and R. Strasser, 1999: Storm-scale numerical weather prediction for commercial and military aviation. Part I: Results from operational tests in 1998. Preprints, *Eighth Conf. on Aviation, Range, and Aerospace Meteorology,* Dallas, TX, Amer. Meteor. Soc., 209–211.

Colle, B. A., and C. F. Mass, 1996: An observational and modeling study of the interaction of low-level southwesterly flow with the Olympic Mountains during COAST IOP 4. *Mon. Wea. Rev.,* **124,** 2152–2175.

——, and ——, 2000: The 5–9 February 1996 flooding event over the Pacific Northwest: Sensitivity studies and evaluation of the MM5 precipitation forecast. *Mon. Wea. Rev.,* **128,** 593–617.

——, K. J. Weatrick, and C. F. Mass, 1999: Evaluation of MM5 and Eta-10 precipitation forecast over the Pacific Northwest during the cool season. *Wea. Forecasting,* **14,** 137–154.

Courtier, P., C. Freydier, J.-F. Geleyn, F. Rabier, and M. Rochas, 1991: The ARPEGE project at Mèteo-France. *Proc. ECMWF Workshop on Numerical Methods in Atmospheric Models,* Reading, United Kingdom, ECMWF.

Droegemeier, K. K., and Coauthors, 1996: The 1996 CAPS spring operational forecasting period: Realtime storm-scale NWP. Part I: Goals and methodology. Preprints, *11th Conf. on Numerical Weather Prediction,* Norfolk, VA, Amer. Meteor. Soc., 294–296.

Falkovich, A., E. Kalnay, S. Lord, and M. B. Mathur, 2000: A new method of observed rainfall assimilation in forecast models. *J. Appl. Meteor.,* **39,** 1282–1298.

Gaudet, B., and W. R. Cotton, 1998: Statistical characteristics of a real-time precipitation forecasting model. *Wea. Forecasting,* **13,** 966–982.

Janiskova, M., 2001: Preparatory studies for the use of observations from the Earth radiation mission in NWP. ESA Contract Rep. 13151/98/NL/GD, 79 pp.

Koch, S. E., A. Aksakal, and J. T. McQueen, 1997: The influence of mesoscale humidity and evapotranspiration fields on a model forecast of a cold-frontal squall line. *Mon. Wea. Rev.,* **125,** 384–409.

Kristjánsson, J. E., 1992: Initialization of cloud water in a numerical weather prediction model. *Meteor. Atmos. Phys.,* **50,** 21–30.

Lin, Y.-L., R. D. Farley, and H. D. Orville, 1983: Bulk parameterization of the snow field in a cloud model. *J. Climate Appl. Meteor.,* **22,** 1065–1092.

Mounier, J., 1964: La saison pluviométrique indigente dans les régions océaniques du Sud-Ouest de l'Europe, Bretagne et Galice. *Norois,* **11,** 261–282.

——, 1979: La diversité des climats oceániques de la Península Iberique. *La Meteorologie,* **106,** 205–227.

Powers, J. G., and K. Gao, 2000: Assimilation of DMSP and TOVS satellite soundings in a mesoscale model. *J. Appl. Meteor.,* **39,** 1727–1741.

Rogers, E. R., T. L. Black, D. G. Deaven, G. J. DiMego, Q. Zhao, M. Baldwin, N. W. Junker, and Y. Lin, 1996: Changes to the operational ''early'' Eta analysis/forecast system at the National Centers for Environmental Prediction. *Wea. Forecasting,* **11,** 391–413.

Sandvik, A. D., 1998: Implementation and validation of a condensation scheme in a nonhydrostatic mesoscale model. *Mon. Wea. Rev.,* **126,** 1882–1905.

Schaefer, J. T., 1990: The critical success index as an indicator of warning skill. *Wea. Forecasting,* **5,** 570–575.

Tao, W.-K., and J. Simpson, 1993: Goddard cumulus ensemble model. Part I: Model description. *Terr. Atmos. Ocean Sci.,* **4,** 35–72.

——, ——, and M. McCumber, 1989: An ice–water saturation adjustment. *Mon. Wea. Rev.,* **117,** 231–235.

Xue, M., K. K. Droegemeier, V. Wong, A. Shapiro, and K. Brewster, 1995: ARPS version 4.0 user's guide. Tech. Doc., Center for Analysis and Prediction of Storms, 380 pp. [Available from CAPS, The University of Oklahoma, 100 E. Boyd St., Norman, OK 73019.]

——, and Coauthors, 1996: The 1996 CAPS spring operational forecasting period: Realtime storm-scale NWP. Part II: Operational summary and examples. Preprints, *11th Conf. on Numerical Weather Prediction,* Norfolk, VA, Amer. Meteor. Soc., 297–300.

——, K. K. Droegemeier, and V. Wong, 2000: The Advanced Regional Prediction System (ARPS)—a multiscale nonhydrostatic atmospheric simulation and prediction tool. Part I: Model dynamics and verification. *Meteor. Atmos. Phys.,* **75,** 161–193.

——, and Coauthors, 2001: The Advanced Regional Prediction System (ARPS)—a multi-scale nonhydrostatic atmospheric simulation and prediction tool. Part II: Model physics and applications. *Meteor. Atmos. Phys.,* **76,** 143–166.

Zapotocny, T. H., and Coauthors, 2000: Study of the sensitivity of the data assimilation system. *Wea. Forecasting,* **15,** 603–621.

Zhang, J., 1999: Moisture and diabatic initializations based on radar and satellite observations. Ph.D. dissertation, University of Oklahoma, 194 pp.

——, F. Carr, and K. Brewster, 1998: ADAS cloud analysis. Preprints, *12th Conf. on Numerical Weather Prediction,* Phoenix, AZ, Amer. Meteor. Soc., 185–188.